

# Integrated Multiscale Domain Adaptive YOLO

Mazin Hnewa, *Student Member, IEEE* and Hayder Radha, *Fellow, IEEE*

**Abstract**—The area of domain adaptation has been instrumental in addressing the domain shift problem encountered by many applications. This problem arises due to the difference between the distributions of source data used for training in comparison with target data used during realistic testing scenarios. In this paper, we introduce a novel MultiScale Domain Adaptive YOLO (MS-DAYOLO) framework that employs multiple domain adaptation paths and corresponding domain classifiers at different scales of the recently introduced YOLOv4 object detector. Building on our baseline multiscale DAYOLO framework, we introduce three novel deep learning architectures for a Domain Adaptation Network (DAN) that generates domain-invariant features. In particular, we propose a Progressive Feature Reduction (PFR), a Unified Classifier (UC), and an Integrated architecture. We train and test our proposed DAN architectures in conjunction with YOLOv4 using popular datasets. Our experiments show significant improvements in object detection performance when training YOLOv4 using the proposed MS-DAYOLO architectures and when tested on target data for autonomous driving applications. Moreover, MS-DAYOLO framework achieves an order of magnitude real-time speed improvement relative to Faster R-CNN solutions while providing comparable object detection performance.

**Index Terms**—Object Detection, Domain adaptation, Adversarial training, Domain shift, MultiScale.

## I. INTRODUCTION

CONVOLUTIONAL Neural Networks (CNNs) have been achieving exceedingly improved performance for object detection in terms of classifying and localizing a variety of objects in a scene. [1]–[7]. However, under a domain shift, when the testing data has a different distribution from the training data distribution, the performance of state-of-the-art object detection methods, drops noticeably and sometimes significantly. Such domain shift could occur due to capturing the data under different lighting or weather conditions, or due to viewing the same objects from different viewpoints leading to changes in object appearance and background. For example, training data used for autonomous vehicles is normally captured under favorable clear weather conditions whereas testing could take place under more challenging weather (*e.g.* rain, fog). Consequently, methods fail to detect objects as shown in the examples of Figure 1(b). In that context, the domain under which training is done is known as the *source domain* while the new domain under which testing is conducted is referred to as the *target domain*.

One of the challenges that aggravates the domain shift problem is the lack of target domain data, and especially annotated data. This led to the emergence of the area of

This work has been supported by the Ford Motor Company under the Ford-MSU Alliance Program.

Mazin Hnewa and Hayder Radha are with Department of Electrical and Computer Engineering, Michigan State University, East Lansing, MI 48824 USA. (e-mail: (mazin, radha)@msu.edu).



Fig. 1. Visual detection examples using the original YOLOv4 method on: (a) clear images and (b) foggy images. (c) Our proposed MS-DAYOLO applied onto foggy images. The images are from the Cityscapes [8] and Foggy Cityscapes [9] datasets.

*domain adaptation* [10]–[15], which has been widely studied to solve the problem of domain shift without the need to annotate data for new target domains. In general, domain adaptation solutions have relied on adversarial networks and other strategies that are designed to generate domain-invariant features. Consequently, the particular domain adaptation solution used is influenced greatly by the underlying object detection method architecture. In that context, within the area of object detection, domain adaptation has been studied rather extensively for Faster R-CNN object detection and its variants [16]–[21]. However, other popular object detection schemes, and in particular YOLO-based architectures, have received little or no attention.

In this paper, we propose novel domain adaptation architectures for the YOLOv4 object detector. In particular, we introduce four new *MultiScale Domain Adaptive YOLO* (MS-DAYOLO) architectures that promote multiscale domain adaptation for the feature extraction stage and progressive channel reduction strategies for domain classifiers. The proposed MS-DAYOLO framework achieves significant improvements over YOLOv4 as shown in the examples of Figure 1(c). MS-

DAYOLO achieves an order of magnitude real-time speed improvement relative to Faster R-CNN solutions while providing comparable and in some instances superior object detection performance. In particular, the main contributions of this paper can be summarized as follows:

- 1) **Baseline Multiscale DAYOLO:** We introduce a Multiscale Domain Adaptive YOLO (MS-DAYOLO) architecture that supports domain adaptation at different layers of the feature extraction stage within the YOLOv4 backbone network. The MS-DAYOLO architecture, which includes a Domain Adaptive Network (DAN) with multiscale feature inputs and multiple domain classifiers, represents our baseline domain adaptive YOLO framework. It is important to highlight that we have recently introduced the proposed baseline architecture in [22]. Here, we build on this prior work by: (a) introducing three new novel MS-DAYOLO architectures, (b) presenting significantly improved and new performance results relative to the baseline performance, and (c) conducting new and more extensive simulation and ablation studies.
- 2) **Progressive Feature Reduction, Unified Classifier, and Integrated Multiscale DAYOLO:** Building on our baseline MS-DAYOLO framework, we propose three novel domain adaptation architectures that further improve YOLOv4 object detection performance when tested on challenging target data. These architectures are: (a) Progressive Feature Reduction, (b) Unified Classifier, and (c) Integrated MS-DAYOLO framework that combines the benefits of the other two architectures. The corresponding DAN networks for these architectures are explained in detail later in this paper.
- 3) We conducted extensive experiments using the Cityscapes, KITTI, and Waymo datasets. These experiments show that our proposed MS-DAYOLO framework provides significant improvements to the performance of YOLOv4 when tested on the target domain. We also show that MS-DAYOLO provides comparable and sometimes superior object detection performance relative to state-of-the-art approaches that are based on Faster R-CNN object detector. As mentioned above, our proposed MS-DAYOLO architectures achieve this level of state-of-the-art performance while providing an order of magnitude improvements in terms of computational complexity when compared to Faster R-CNN based solutions.

The remainder of this paper is organized as follows. Section II briefly highlights related work. Section III describes the proposed multiscale domain adaptive framework for YOLO object detector in detail, including the novel architectures for domain adaptive network. Section IV provides experimental results of the proposed framework with analysis and discussion. Finally, section V concludes the paper with a summary of the key findings of our work.

## II. RELATED WORK

In general, state-of-the-art CNN based object detection models can be classified into two groups: one-stage and two-stage

based methods. One-stage object detectors predict bounding boxes of objects and class probabilities associated with these objects directly from a full image in single computation via a unified neural network. The most well-known models of one-stage object detectors are YOLO [5], [23]–[25], SSD [4], and RetinaNet [6]. On the other hand, two-stage object detectors generate proposal bounding boxes that potentially have an object using Region Proposal Network (RPN) in the first stage. Then, the proposals are fed to a second stage where cropped features are used to classify objects and fine-tune the bounding boxes. The most well-known models of two-stage object detectors are the R-CNN [1] series, including Fast R-CNN [2], Faster R-CNN [3], R-FCN [7], and Mask R-CNN [26].

Recently, unsupervised domain adaptation has been used to improve the performance of object detection due to domain shift [27]. It attempts to learn a robust object detector using labeled data from the source domain and unlabeled data from the target domain. Domain adaptation approaches for object detection can mainly be classified into reconstruction based and adversarial-based solutions [27]. Reconstruction based domain adaptation attempts to improve the performance of an object detector for target domain by using image-to-image translation models [28]–[32]. In particular, it utilizes image-to-image translation methods to generate artificial (fake) samples of the target domain from the corresponding source labeled samples. Consequently, translating labeled source data into corresponding target data will help in the training of an object detector in a target domain; and this should improve the performance of object detection in that domain.

In adversarial-based, a domain discriminator is trained to classify whether a data point is from the source or target domain, while the feature extractor of the object detector is trained to confuse the domain discriminator [33]. Consequently, the feature extractor generates domain invariant features as a result of this training strategy. Many adversarial-based domain adaptation methods have been proposed for the Faster R-CNN object detector [16]–[21], [34]–[36]. The state-of-the-art approach of adversarial-based domain adaptation is Domain Adaptive Faster R-CNN [16]. Subsequently, many other approaches were proposed. For example, He and Zhang [20] proposed multiple adversarial submodules for both domain and proposal features alignment. Furthermore, Zhao *et al.* [35] proposed a collaborative self-training method that can propagate the loss gradient through the whole detection network, and mutually enhance the region proposal network and the region proposal classifier. In addition, Xu *et al.* [36] utilized elaborate prototype representations to achieve category-level domain alignment.

It is worth noting that most previous approaches for domain adaptation object detection, used Faster R-CNN as the base detector. Despite its popularity, Faster R-CNN suffers from a long inference time to detect objects. As a result, it is arguably not the optimal choice for time-critical, real-time applications such as autonomous driving. On the other hand, one-stage object detectors, and in particular YOLO, can operate quite fast, even much faster than real-time, and this makes them invaluable for autonomous driving and similar time-critical

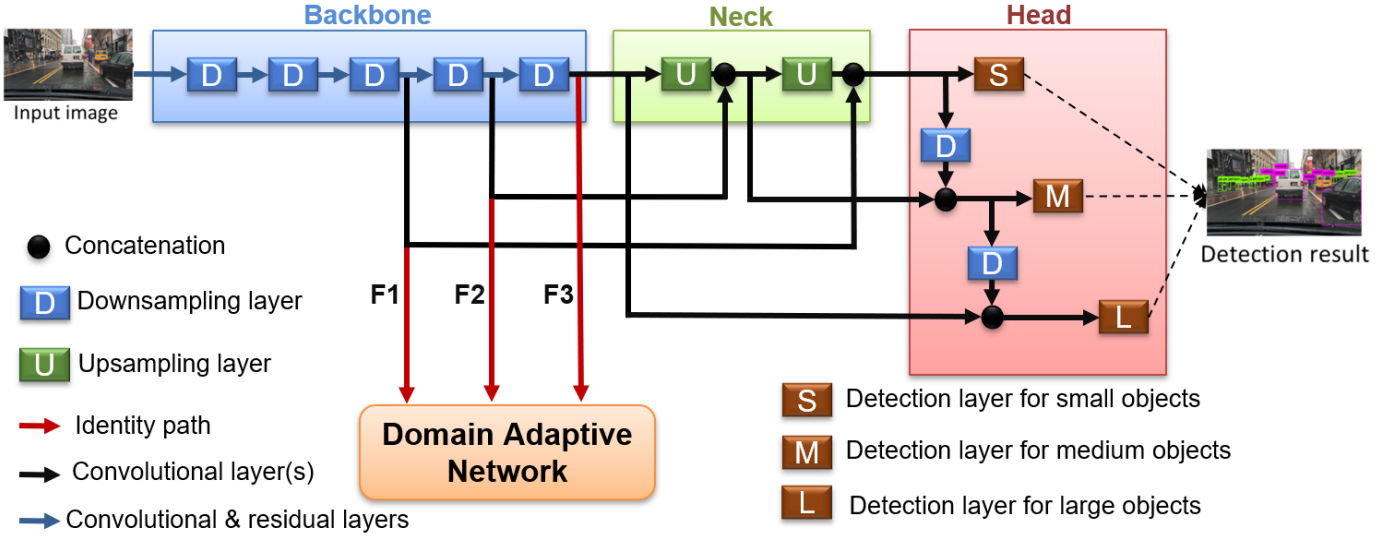


Fig. 2. Architecture of YOLOv4 with domain adaptation network (DAN) to develop domain adaptive YOLO. The details architectures of DAN are shown in Figure 3.

applications. Furthermore, domain adaptation for the family of YOLO architectures, has received virtually no attention. Besides the computational advantage of YOLO, the latest version, YOLOv4, has many salient improvements and its object detection performance has improved rather significantly relative to prior YOLO architectures and more important in comparison to Faster R-CNN. All of these factors motivated our focus on the development of a new domain adaptation framework for YOLOv4.

### III. PROPOSED MULTISCALE DOMAIN ADAPTIVE YOLO

YOLOv4 [25] has been released recently as the latest version of the family of the YOLO object detectors. Relative to its predecessor, YOLOv4 has incorporated many new revisions and novel techniques to improve the overall detection accuracy. YOLOv4 has three main parts: backbone, neck, and head as shown in Figure 2. The backbone is responsible for extracting multiple layers of features at different scales. The neck collects these features from three different scales of the backbone using upsampling layers and feeds them to the head. Finally, the head predicts bounding boxes surrounding objects as well as class probabilities associated with each bounding box.

The backbone (*i.e.* feature extractor) represents a major module of the YOLOv4 architecture, and we believe that it makes a significant impact on the overall performance of the detector. In addition to many convolutional layers, it has 23 residual blocks [37], and five downsampling layers to extract critical layers of features that are used by the subsequent detection stages. Here, we consecrate on the features that are fed to the neck module (F1, F2, and F3 in Figures 2). In particular, our goal is to apply domain adaptation to these three features to make them robust against domain shifts, and hence, have them converge toward domain invariance during domain-adaptation based training. Equally important, these three stages of features have different dimensions due to the successive downsampling layers that progressively reduce the

width and height of features by half while doubling the number of channels. If  $d$  is the width of the feature at the first scale (F1), then the dimensions of the three stages of features are: F1:  $d \times d \times 256$ , F2:  $\frac{d}{2} \times \frac{d}{2} \times 512$ , and F3:  $\frac{d}{4} \times \frac{d}{4} \times 1024$ .

#### A. Domain Adaptive Network for YOLO

The proposed Domain Adaptive Network (DAN) is attached to the YOLOv4 object detector only during training in order to learn domain invariant features. Indeed, YOLOv4 and DAN are trained in an end-to-end fashion. For inference, and during testing, domain-adaptive trained weights are used in the original YOLOv4 architecture (without the DAN network). Therefore, our proposed framework will not increase the underlying detector complexity during inference, which is an essential factor for many real-time applications such as autonomous driving.

DAN uses the three distinct scale features of the backbone that are fed to the neck as inputs. It has several convolutional layers to predict the domain class (either source or target). Then, domain classification loss ( $\mathcal{L}_{dc}$ ) is computed via binary cross entropy as follows:

$$\mathcal{L}_{dc} = -\frac{1}{N} \sum_{i,x,y} [t_i \ln p_i^{(x,y)} + (1 - t_i) \ln(1 - p_i^{(x,y)})] \quad (1)$$

Here,  $t_i$  is the ground truth domain label for the  $i$ -th training image, with  $t_i = 1$  for source domain and  $t_i = 0$  for target domain.  $p_i^{(x,y)}$  is predicted domain class probabilities for  $i$ -th training image at location  $(x,y)$  of the feature map.  $N$  represents the total number of images in a batch multiplied by the total number of elements in the feature map.

DAN is optimized to differentiate between the source and target domains by minimizing this loss. On the other hand, the backbone is optimized to maximize the loss to learn domain invariant features. Thus, features of the backbone should

be indistinguishable for the two domains. Consequently, this should improve the performance of object detection for the target domain.

To solve the joint minimization and maximization problem, we employ the adversarial learning strategy [33]. In particular, we achieve this contradictory objective by using a Gradient Reversal Layer (GRL) [12], [15] between the backbone and the DAN network. GRL is a bidirectional operator that is used to realize two different optimization objectives. In the feed-forward direction, the GRL acts as an identity operator. This leads to the standard objective of minimizing the classification error when performing local backpropagation within DAN. On the other hand, for backpropagation toward the backbone network, the GRL becomes a negative scalar ( $\lambda$ ). Hence, in this case, it leads to maximizing the binary-classification error; and this maximization promotes the generation of domain-invariant features by the backbone.

To compute the detection loss ( $\mathcal{L}_{det}$ ) [25], only source images are used because they are annotated with ground-truth objects. Consequently, all three parts of YOLOv4 (*i.e.* backbone, neck and head) are optimized via minimizing  $\mathcal{L}_{det}$ . On the other hand, both source labeled images and target unlabeled images are used to compute the domain classification loss ( $\mathcal{L}_{dc}$ ) which is used to optimize DAN via minimizing it, and the backbone via maximizing it. As a result, both  $\mathcal{L}_{det}$  and  $\mathcal{L}_{dc}$  are used to optimize the backbone. In other words, the backbone is optimized by minimizing the following total loss:

$$\mathcal{L}_t = \mathcal{L}_{det} + \lambda \mathcal{L}_{dc} \quad (2)$$

where  $\lambda$  is a negative scalar of GRL that balances a trade-off between the detection loss and domain classification loss. In fact,  $\lambda$  controls the impact of DAN on the backbone.

## B. DAN Architectures

We developed various architectures for the Domain Adaptive Network (DAN) as shown in Figure 3 to explore and gain insight into the impact of different components on achieving improved performance for the target domain. Under all of our architectures, we employ a multiscale strategy that connects the three features F1, F2, and F3 of the backbone to the DAN through three corresponding GRLs. Other than this common multiscale strategy, the proposed DAN architectures differ from each other as explained below.

**a- Multiscale Baseline** : Instead of applying domain adaptation for only the final scale of the feature extractor as done in the Domain Adaptive Faster R-CNN architecture [16], we develop domain adaptation for three scales separately to solve the gradient vanishing problem. In other words, applying domain adaptation only to the final scale (F3) does not make a significant impact on the previous scales (F1 and F2) due to the gradient vanishing problem as there are many layers between them. As a result, we apply domain adaptation to all scales as shown in Figure 3 (a). For each scale, there are two convolutional layers after GRL, the first one reduces the feature channels by half, and the second one predicts the domain class probabilities. Finally, a domain classifier layer is used to compute the domain classification loss.

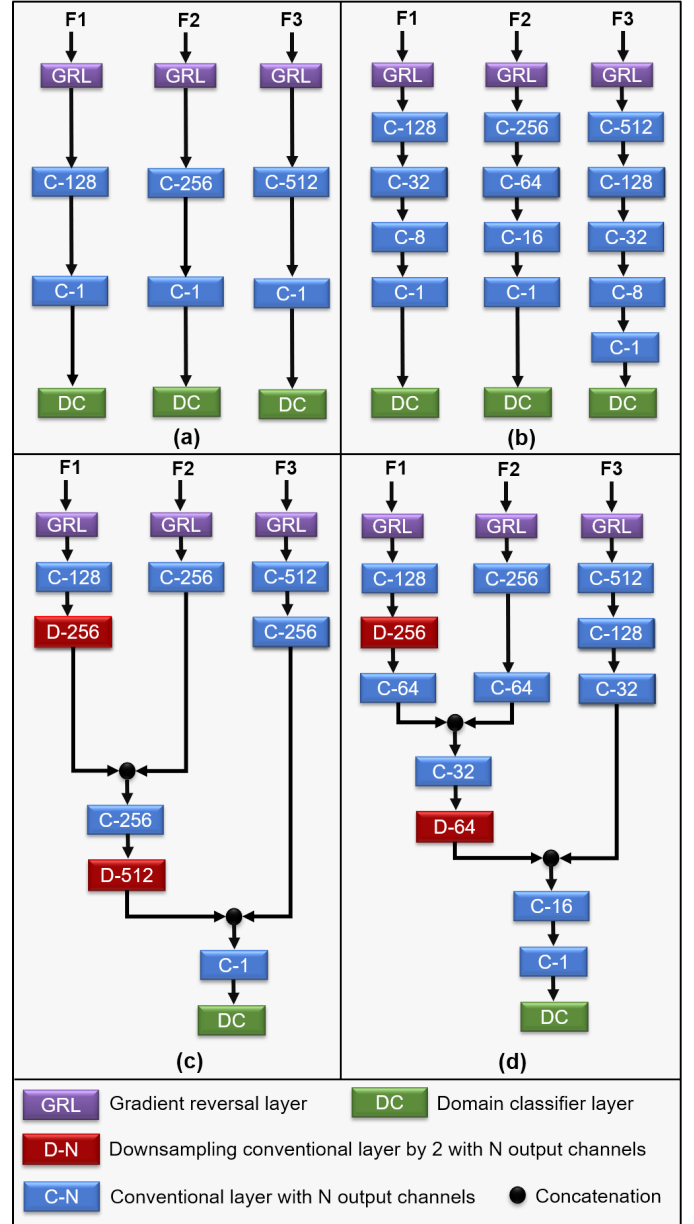


Fig. 3. Proposed architectures for the Domain Adaptive Network (DAN): (a) Baseline, (b) Progressive Feature Reduction (PFR), (c) Unified Classifier (UC), (d) Integrated. F1, F2, and F3 are features of the backbone network that are fed to the neck.

**b- Progressive Feature Reduction (PFR)**: As shown in Figure 3(a), the baseline architecture reduces the feature vector size resulting from the YOLOv4 backbone into a single-value feature (scalar) rather abruptly through two stages of neural networks. This simple two-stage DAN aims at generating a single feature value that serves as an input into the domain classifier. The fact that the domain classifier requires a single feature value is inherent in the binary nature of the classifier that simply needs to classify the image data into either source domain or target domain. Meanwhile, and due to the adversarial strategy used here, the above Baseline domain adaptation network is competing with the significantly more complex network of the backbone as shown in Figure 2. We

observed that this mismatch between the simplistic baseline DAN architecture and the complex backbone network could compromise the domain adaptation performance. Thus, the DAN network may not be sufficiently powerful to distinguish between the source and target domains since the complex backbone network can easily confuse (and trick) the DAN network. To mitigate this mismatch, we increase the number of convolutional layers for each scale by progressively reducing the feature channels as shown in Figure 3(b). This progressive reduction of feature channels helps the DAN network to compete more efficiently against the more complex backbone. As a result, the extracted features by the backbone network will be more domain invariant.

Therefore, while the baseline architecture reduces the number of the feature channels using two stages of neural networks, our proposed progressive-feature-reduction employs four or five stages depending on the original feature size. In particular, for feature vectors F1 and F2, we employ four stages of neural networks that progressively reduce the feature vector size from 128 and 256, respectively, toward a single-feature scalar value, which is all that is required as an input for the binary domain classifier. For feature vector F3, we employ a five-stage neural network DAN to progressively reduce the backbone feature vector toward the scalar feature value. It is important to highlight the following regarding the proposed progressive-feature-reduction architecture. It is possible to employ a larger number of stages of progressive reduction than the number of stages we employed in our architecture shown in Figure 3(b). However, based on our experience, increasing the number of stages beyond four or five stages does not necessarily improve the overall performance.

**c- Unified Classifier (UC):** Under the multiscale baseline and Progressive Feature Reduction architectures, each scale has its own distinct domain classifier. This multi-classifier strategy may lead to inconsistency among scales. For example, a domain classifier at one scale may classify an image patch as a source data, while a domain classifier at another scale may classify the same image patch as originating from the target domain. (Examples of this inconsistency are shown later in the Experiments section.) To address this potential inconsistency, we propose to use a single (unified) domain classifier that combines the feature vectors from all scales as shown in Figure 3(c). It is important to highlight the following about the proposed Unified Classifier (UC) domain adaptive network:

- 1) We use downsampling convolutional layers to match the size of features at different scales. For example, in order to combine the feature vectors resulting from the F1 and F2 scales of the backbone, we add a downsampling stage to the F1 scale and concatenate the resulting vector with the feature vector from F2. This strategy maintains the multiscale attribute of our domain adaptive network while targeting a unified domain classifier architecture.
- 2) Furthermore, we concatenate features at different scales in a way to make each scale contributes equally in terms of the number of feature channels. In other words, each feature scale equally contributes in the prediction of the domain class probabilities.

**d- Integrated:** It is important to note that the above two improvements, progressive feature reduction (PFR) and unified classifier (UC), have been applied directly and separately to the multiscale baseline architecture. Consequently, to gain the benefits of both, the progressive feature reduction and unified domain classifier strategies, we integrate them in one network as shown in Figure 3(d). In principle, we have developed the network by complementing the unified-classifier architecture (Figure 3(c)) with additional stages of convolutional layers to achieve a more progressive reduction in feature channel sizes. This is evident by comparing the two architectures shown in Figures 3(c) and 3(d).

## IV. EXPERIMENTS

In this section, we evaluate our proposed domain adaptive YOLO framework and the proposed MS-DAYOLO architectures. We modified the official source code of YOLOv4 that is based on the darknet platform<sup>1</sup>, and we developed a new code to implement our proposed methods.

### A. Setup

For training, we used the default settings and hyperparameters that were used in the original YOLOv4 [25]. The network is initialized using the pre-trained weights file. The training data includes two sets: source data that has images and their annotations (bounding boxes and object classes), and target data without annotation. Each batch has 64 images, 32 from the source domain and 32 from the target domain. Based on prior works [16], [17], [20] and on our experience using trial and error, we set  $\lambda = 0.1$  for all experiments.

For evaluation, we report Average Precision (AP) for each class as well as mean average precision (mAP) with a threshold of 0.5 [38] using testing data that has labeled images of the target domain. We have followed other prior domain adaptive object-detection works that use the same threshold value of 0.5. We compare our proposed method with the original YOLOv4 and other state-of-the-art domain adaptation approaches that are based on Faster R-CNN object detector [3], all applied to the same target domain validation set.

### B. Results

*1) Adverse Weather Adaptation:* Domain shift due to changes in weather conditions is one of the most prominent reasons for the discrepancy between the source and target domains. Reliable object detection systems in different weather conditions are essential for many critical applications such as autonomous driving. As a result, we focus on presenting the evaluation results of our proposed MS-DAYOLO framework by studying domain shifts under challenging weather conditions for autonomous driving. To achieve this, we use three different driving datasets: Cityscapes [8], Foggy Cityscapes [9], Waymo [39].

**Clear → Foggy:** We discuss the ability of our proposed method to adapt from clear to foggy weather using driving datasets: Cityscapes [8] and Foggy Cityscapes [9] as has been

<sup>1</sup><https://github.com/AlexeyAB/darknet>

TABLE I

QUANTITATIVE RESULTS OF DOMAIN ADAPTATION FOR THE CLEAR  $\rightarrow$  FOGGY EXPERIMENT OF THE CITYSCAPES DATASET. THE MS-DAYOLO USES YOLOv4 OBJECT DETECTOR [25], WHILE THE OTHER METHODS USE FASTER R-CNN OBJECT DETECTOR [3]. \*THE RESULTS ARE REPORTED FROM [41] AND [43]. THE INFERENCE TIME IS MEASURED IN FRAME PER SECOND (FPS) USING NVIDIA GeForce GTX 1080 Ti GPU.

Method	Backbone	Person	Rider	Car	Truck	Bus	Train	Mcycle	Bicycle	mAP	FPS
DAF (CVPR'18) [16]	VGG16	25.0	31.0	40.5	22.1	35.3	20.2	20.0	27.1	27.6	6.2
MAF (ICCV'19) [20]		28.2	39.5	43.9	23.8	39.9	33.3	29.2	33.9	34.0	
iFAN (AAAI'20) [34]		32.6	40.0	48.5	27.9	45.5	31.7	22.8	33.0	35.3	
CT (ECCV'20) [35]		32.7	44.4	50.1	21.7	45.6	25.4	30.1	36.8	35.9	
PDA (WACV'20) [36]		36.0	45.5	54.4	24.3	44.1	25.8	29.1	35.9	36.9	
DAF (CVPR'18) [16]*	ResNet50	29.2	40.4	43.4	19.7	38.3	28.5	23.7	32.7	32.0	3.7
MTOR (CVPR'19) [41]		30.6	41.4	44.0	21.9	38.6	40.6	28.3	35.6	35.1	
GPA (CVPR'20) [43]		32.9	<b>46.7</b>	54.1	24.7	45.7	41.1	<b>32.4</b>	<b>38.7</b>	39.5	
YOLOv4		31.6	38.3	46.9	23.9	39.9	20.1	16.8	30.3	31.0	48.2
MS-DAYOLO	Baseline	38.6	45.5	55.9	22.8	45.6	32.5	28.8	36.5	38.3	
	PFR	38.5	46.5	56.5	27.6	48.7	38.5	26.4	38.4	40.1	
	UC	39.3	45.0	<b>57.0</b>	<b>29.9</b>	48.0	36.6	30.2	36.4	40.3	
	Integrated	<b>39.6</b>	46.5	56.5	28.9	<b>51.0</b>	<b>45.9</b>	27.5	36.0	<b>41.5</b>	
Oracle		42.4	49.5	63.6	37.6	59.8	47.1	31.1	39.9	46.3	

done by many recent works in this area [16]–[21], [40]–[42]. The Cityscapes training set has 2975 labeled images that are used as source domain. Similarly, the Foggy Cityscapes training set also has 2975 images, but without annotations, and are used as the target domain. Original YOLOv4 is trained using the source domain data only. While MS-DAYOLO is trained using both source and target domain data. The Foggy Cityscapes validation set has 500 labeled images which are used for testing and evaluation. Because the Foggy Cityscapes training set is annotated, we are able to train the original YOLOv4 with this set to show the ideal performance (oracle).

Table I summarizes the performance results. Based on these results, all of the architectures of our proposed framework outperform the original YOLOv4 approach by a significant margin. Moreover, the proposed integrated architecture achieves the best overall performance in terms of mAP. Although the GPA method has slightly better results than the proposed integrated architecture in terms of AP for some classes, the integrated MS-DAYOLO achieves the best overall performance in term of mAP, and it is significantly faster than GPA in inference time. It is worth noting that the proposed integrated architecture achieves significant improvements relative to the original YOLOv4, and it almost reaches the performance of the ideal (oracle) scenario, especially for some object classes in terms of average precision. Figure 1 shows examples of detection results of the proposed method as compared to the original YOLOv4.

**Sunny  $\rightarrow$  Rainy:** we present results for applying YOLOv4 and our MS-DAYOLO framework on the Waymo dataset [39], which includes two sets of visual data that are designated as "sunny" and "rainy". We extracted 14319 "sunny weather" labeled images for the source data, and 13004 "rainy weather" unlabeled images to represent the target data. As before, the original YOLOv4 is trained using only source data (*i.e.* labeled sunny images). Meanwhile, our proposed MS-DAYOLO is trained using both source and target data (*i.e.* labeled sunny images and unlabeled rainy images). In addition, we extracted 1676 labeled images from the rainy-weather data for testing and evaluation. It is important to note the following key observations regarding the Waymo datasets: (a) The designa-



Fig. 4. Examples of training images of Waymo dataset [39]. Images in the top row are tagged as being captured in sunny weather, while images in the bottom row are tagged as being captured in rainy weather. It is obvious that the domain shift between sunny and rainy images is not very significant.

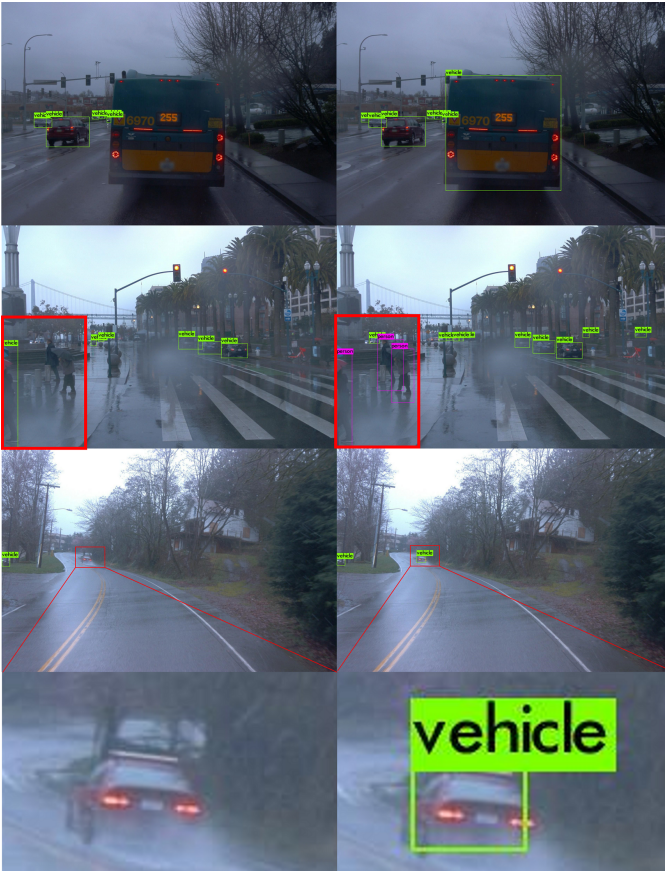
TABLE II

QUANTITATIVE RESULTS OF DOMAIN ADAPTATION FOR THE SUNNY  $\rightarrow$  RAINY EXPERIMENT OF THE WAYMO DATASET.

Method		Person	Vehicle	mAP
YOLOv4		38.56	55.41	46.99
MS-DAYOLO	Baseline	39.97	55.37	47.67
	PFR	39.75	56.34	48.05
	UC	39.42	56.66	48.04
	Integrated	<b>40.03</b>	<b>56.97</b>	<b>48.50</b>

tions "sunny" and "rainy" images have been determined by the providers of the Waymo dataset. (b) From our extensive experience in working with this data, the distinction between sunny and rainy image samples is quite subjective, and in many cases, one can argue that a "rainy" image sample should be labeled as "sunny" or vice versa. Consequently, the domain shift between the two domains, which are designated as "sunny" and "rainy", is not very significant as shown in the examples of Figure 4. This is crucial since training the original YOLOv4 using the Waymo "sunny" dataset effectively covers a large number of "rainy" testing samples that fall within the source "sunny" domain. Nevertheless, we opted to follow the dataset designations with the aim of evaluating any potential improvements that the proposed MS-DAYOLO framework may provide.

The results are summarized in Table II. It is clear that the



(a) YOLOv4

(b) Our MS-DAYOLO

Fig. 5. Visual detection examples of the sunny  $\rightarrow$  rainy experiment using (a) the original YOLOv4, and (b) Our proposed Integrated MS-DAYOLO applied onto labeled rainy images extracted from the Waymo dataset [39].

MS-DAYOLO framework still provided good improvements despite the fact that, in this case, the two domains, sunny and rainy, have a significant overlap. This could explain why the improvements are not as salient as the improvements achieved when applying MS-DAYOLO on the Cityscapes data, which consisted of two clearly distinct domains as shown in the examples of Figure 1. Moreover, and similar to the clear  $\rightarrow$  foggy experiment, we observe that the proposed Progressive Feature Reduction (PFR), Unified Classifier (UC), and Integrated architectures improve the detection performance relative to the baseline architectures when applied to the Waymo dataset. For this experiment, we do not report the performance of other domain adaptive object detection methods that are based on Faster R-CNN because none of these methods reported or used the Waymo dataset for the sunny  $\rightarrow$  rainy domain-shift scenario. Figure 5 shows examples of detection results of the proposed Integrated MS-DAYOLO framework as compared to the original YOLOv4. In addition, Figure 6 shows examples of detection results that the integrated architecture succeeds in detecting objects while the baseline architecture fails to detect the same objects. Furthermore, Figure 7 shows examples where the baseline architecture suffers from false positive cases, while the integrated one eliminates these false positives, which contribute to its improved performance.



(a) Baseline MS-DAYOLO

(b) Integrated MS-DAYOLO

Fig. 6. Visual detection examples of the sunny  $\rightarrow$  rainy experiment using (a) the baseline architecture, and (b) the integrated architecture of MS-DAYOLO applied onto the rainy images extracted from the Waymo dataset [39]. The baseline MS-DAYOLO fails to detect pedestrians crossing the street in the top two images, and cars in the bottom two images, while the integrated MS-DAYOLO successfully detects these objects.

2) *Cross Camera Adaptation*: Domain shift can occur between different real visual datasets captured by different driving vehicles equipped with different cameras even if these visuals are taken under similar weather conditions. Such domain shift is usually driven by different camera setups leading to a shift in image quality and resolution. Moreover, such datasets are usually captured in various locations, which have different views and driving environments. All these factors lead to domain disparity between datasets. Under this experiment, we evaluate the performance of our MS-DAYOLO framework for domain adaptation between two real driving datasets: KITTI [44] and Cityscapes as has been done by many recent works in this area [16], [17], [20], [36], [40]. In particular, the KITTI training set which has 6000 labeled images, is utilized as source data. While the Cityscapes training set which has 2975 images, but without labels, is utilized as target data. The Cityscapes validation set which has 500 labeled images, is used for testing and evaluation.

Table III presents the performance results based on the car AP as has been reported by prior works [16], [17], [20], [36], [40] because it is the only common object class



(a) Baseline MS-DAYOLO (b) Integrated MS-DAYOLO

Fig. 7. Visual detection examples of the sunny  $\rightarrow$  rainy experiment using (a) the baseline architecture, and (b) the integrated architecture of MS-DAYOLO applied onto the rainy images extracted from the Waymo dataset [39]. In these examples, the baseline MS-DAYOLO suffers from instances of false positive, while the integrated MS-DAYOLO eliminates these false positives. **FP**: means false positive.

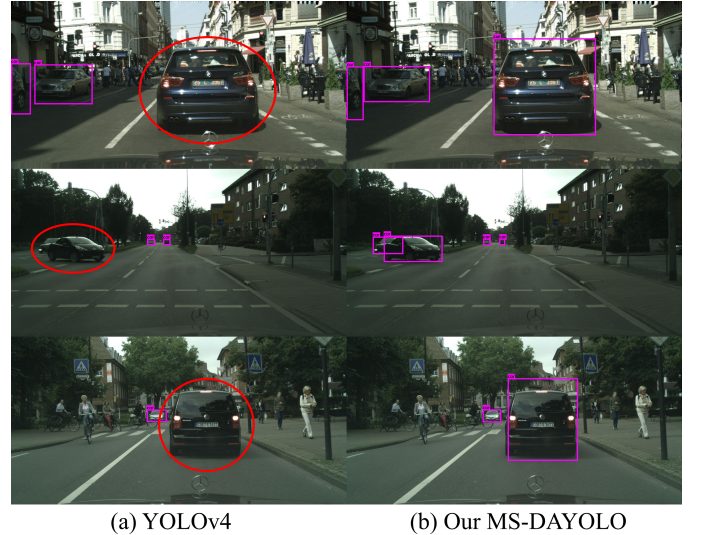
between the two datasets. A clear performance improvement is achieved by our method over the original YOLOv4. We also observe that the proposed Progressive Feature Reduction (PFR), Unified Classifier (UC), and Integrated architectures improve the detection performance relative to the baseline architecture. Although the GPA method outperforms Integrated MS-DAYOLO by a small margin (0.3%), our MS-DAYOLO runs in real-time, and it is significantly faster than GPA in terms of frames per second (FPS), which is essential for time-critical applications. Figure 8 shows visual examples for qualitative comparison of our method with the original YOLOv4. It is obvious from these examples that our approach successfully detects the vehicles in the scenes while the original YOLOv4 fails to detect the same vehicles.

### C. Ablation Study

To show the importance of applying domain adaptation to three distinct scales of the backbone network, we conducted an ablation study for the clear  $\rightarrow$  foggy experiment. First, we applied domain adaptation, separately, to each of the three scales of features that are fed into the neck of the YOLOv4

TABLE III  
QUANTITATIVE RESULTS OF CROSS CAMERA ADAPTATION FROM KITTI TO CITYSCAPES BASED ON AP OF THE CAR CLASS WHICH IS SHARED BETWEEN THE TWO DATASETS. THE MS-DAYOLO USES YOLOV4 OBJECT DETECTOR [25], WHILE THE OTHER METHODS USE FASTER R-CNN OBJECT DETECTOR [3]. \*THE RESULTS ARE REPORTED FROM [43]. THE INFERENCE TIME IS MEASURED IN FRAME PER SECOND (FPS) USING NVIDIA GEFORCE GTX 1080 TI GPU.

Method	Backbone	Car AP	FPS
DAF (CVPR'18) [16]	VGG16	38.5	6.2
MAF (ICCV'19) [20]		41.0	
CT (ECCV'20) [35]		43.6	
PDA (WACV'20) [36]		43.9	
DAF (CVPR'18) [16]*	ResNet50	41.8	3.6
GPA (CVPR'20) [43]		<b>47.9</b>	
YOLOv4		44.5	<b>48.2</b>
MS-DAYOLO	Baseline	45.5	
	PFR	46.8	
	UC	47.3	
	Integrated	47.6	



(a) YOLOv4 (b) Our MS-DAYOLO

Fig. 8. Visual detection examples of the KITTI  $\rightarrow$  Cityscapes experiment for the car class using (a) the original YOLOv4, and (b) Our proposed integrated MS-DAYOLO applied onto the Cityscapes validation set. These examples show that the integrated MS-DAYOLO successfully detects the vehicles in the scenes while the original YOLOv4 fails to detect the same vehicles.

architecture. Also, we applied domain adaptation to different combinations of two scales at a time. Finally, we compared the results with the performance of applying these combinations of the study with the performance of applying our baseline MS-DAYOLO to all three scales as explained in section III-B. Another important aspect of this ablation study is that we wanted to consider objects that have statistically significant numbers of sample data. In that context, because the number of ground-truth objects for some classes (truck, bus, and train) is small (*i.e.* less than 500 in the training set, and 100 in the testing set), the performance measure will be inaccurate for these classes. As a result, we exclude them in this ablation study and compute mAP based on the remaining classes.

Table IV summarizes results of the ablation study. It is clear that based on these results, we can conclude that applying domain adaptation to all three feature scales improves the

TABLE IV  
ABLATION STUDY, ✓ MEANS THAT DOMAIN ADAPTATION IS APPLIED TO THE FEATURE SCALE(S) USING OUR BASELINE MS-DAYOLO.

F1	F2	F3	Person	Rider	Car	Mcycle	Bicycle	mAP
			31.57	38.27	46.93	16.75	30.32	32.77
		✓	36.84	42.84	53.69	24.77	32.35	38.09
	✓		37.08	41.49	54.49	26.22	32.43	38.34
✓			36.28	44.22	53.10	25.81	35.87	39.06
	✓	✓	36.62	42.68	55.70	26.09	33.52	38.92
✓	✓		37.50	42.48	54.53	27.84	34.75	39.43
✓		✓	36.41	<b>46.06</b>	52.19	22.48	34.99	38.43
✓	✓	✓	<b>38.62</b>	45.52	<b>55.85</b>	<b>28.82</b>	<b>36.46</b>	<b>41.05</b>

detection performance on the target domain, and achieves the best result.

#### D. Analysis

In order to show the benefits of Progressive Feature Reduction (PFR) relative to the baseline architecture, we recorded the domain classifier loss of Equation 1 over training iterations for the clear  $\rightarrow$  foggy experiment. Figure 9 shows the classifier loss averaged over the losses of the three domain classifiers, corresponding to features F1, F2, and F3, for both architectures, Baseline and PFR (Figures 3 (a) and (b), respectively) over the first 5K iterations of training.

It is clear from the figure that the average loss under PFR is consistently smaller than the average domain classifier loss under the Baseline, especially after 1.5K iterations. This implies that the proposed PFR architecture can compete with the backbone network in a more meaningful way than the Baseline classifiers can. This gain in domain classifier performance is due to the fact that the PFR network has more convolutional layers than the Baseline. It is important to note that the adversarial strategy aims at tricking or confusing the *best* possible domain classifier. Consequently, it is crucial to develop as good domain classifier as possible, despite the fact that we are trying to trick it in terms of not being able to distinguish between source and target data. Hence, features generated through an adversarial relationship with a more superior domain-classifier should be more domain-invariant. Therefore, training using the PFR network leads to better domain-invariant features than training the baseline network. And, this leads to improving the detection performance on target domain data as shown in Tables I, II and III.

Moreover, to show the benefit of using a unified domain classifier instead of three different domain classifiers, we plot in Figure 10 the losses of the three domain classifiers of the baseline architecture over the first 5K iterations of training for the clear  $\rightarrow$  foggy experiment. We can see that the losses are dissimilar after 1K iterations. This implies inconsistency among the classifiers' performance, which leads to drop in performance. This motivated our objective in employing a unified domain classifier for all three scales. In turn, this led to the UC architecture for improving the detection performance when applied to the target domain data as shown in Tables I, II and III.

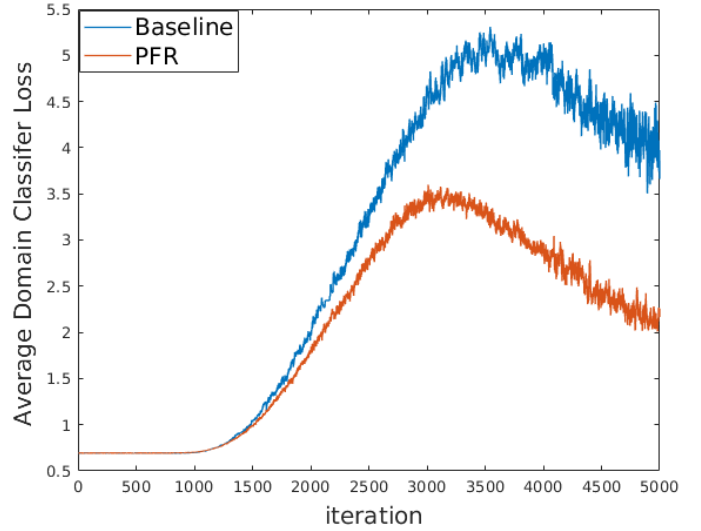


Fig. 9. Average loss of three domain classifiers in Baseline and Progressive Feature Reduction (PFR) architectures over the first 5K iterations of training.

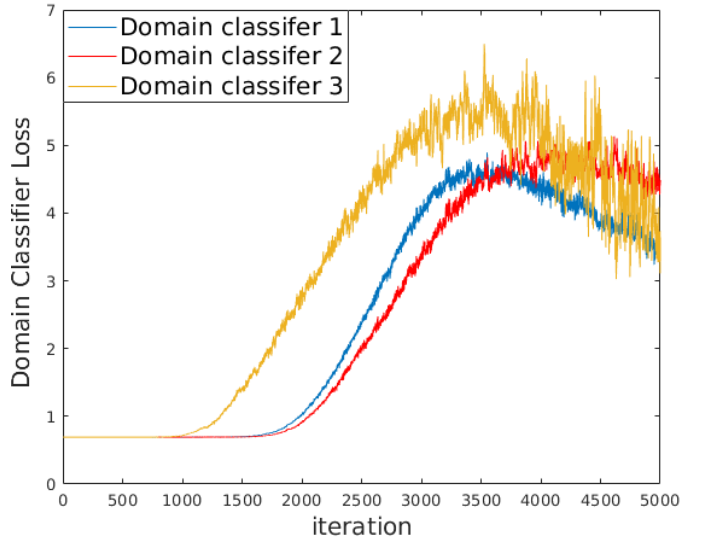


Fig. 10. Losses of three domain classifiers in the Baseline architecture over the first 5K iterations of training.

## V. CONCLUSION

In this paper, we proposed a multiscale domain adaptation framework for the popular state-of-the-art real time object detector YOLO. Specifically, under our MS-DAYOLO architecture, we applied domain adaptation to three different scale features within the YOLO feature extractor that are fed to the next stage. In addition to the baseline architecture of a multiscale domain adaptive network, we developed three various deep learning architectures to produce more robust domain invariant features that reduce the impact of domain shift. The proposed architectures include progressive feature reduction (PFR), unified domain classifier (UC), and the integrated architecture that combines the benefits of progressive-feature reduction and unified classifier strategies for improving the

overall detection performance under the target domain. Based on various experimental results, our proposed MS-DAYOLO framework can successfully adapt YOLO to target domains without annotation. Furthermore, the proposed MS-DAYOLO architectures outperformed state-of-the-art YOLOv4 and other exciting approaches that are based on Faster R-CNN object detector under diverse testing scenarios for autonomous driving applications.

## REFERENCES

- [1] R. Girshick, J. Donahue, T. Darrell, and J. Malik, "Rich feature hierarchies for accurate object detection and semantic segmentation," in *Proceedings of the IEEE conference on computer vision and pattern recognition*, 2014, pp. 580–587.
- [2] R. Girshick, "Fast r-cnn," in *Proceedings of the IEEE international conference on computer vision*, 2015, pp. 1440–1448.
- [3] S. Ren, K. He, R. Girshick, and J. Sun, "Faster r-cnn: Towards real-time object detection with region proposal networks," *IEEE Transactions on Pattern Analysis and Machine Intelligence*, vol. 39, no. 6, pp. 1137–1149, June 2017.
- [4] W. Liu, D. Anguelov, D. Erhan, C. Szegedy, S. Reed, C.-Y. Fu, and A. C. Berg, "Ssd: Single shot multibox detector," in *European conference on computer vision*. Springer, 2016, pp. 21–37.
- [5] J. Redmon, S. Divvala, R. Girshick, and A. Farhadi, "You only look once: Unified, real-time object detection," in *IEEE Conference on Computer Vision and Pattern Recognition (CVPR)*, June 2016, pp. 779–788.
- [6] T.-Y. Lin, P. Goyal, R. Girshick, K. He, and P. Dollár, "Focal loss for dense object detection," in *The IEEE International Conference on Computer Vision (ICCV)*, Oct 2017.
- [7] J. Dai, Y. Li, K. He, and J. Sun, "R-fcn: Object detection via region-based fully convolutional networks," in *Advances in neural information processing systems*, 2016, pp. 379–387.
- [8] M. Cordts, M. Omran, S. Ramos, R. Rehfeld, M. Enzweiler, R. Benenson, U. Franke, S. Roth, and B. Schiele, "The cityscapes dataset for semantic urban scene understanding," in *Proc. of the IEEE Conference on Computer Vision and Pattern Recognition (CVPR)*, 2016.
- [9] C. Sakaridis, D. Dai, and L. Van Gool, "Semantic foggy scene understanding with synthetic data," *International Journal of Computer Vision*, vol. 126, no. 9, pp. 973–992, 2018.
- [10] L. Duan, I. W. Tsang, and D. Xu, "Domain transfer multiple kernel learning," *IEEE Transactions on Pattern Analysis and Machine Intelligence*, vol. 34, no. 3, pp. 465–479, 2012.
- [11] B. Kulis, K. Saenko, and T. Darrell, "What you saw is not what you get: Domain adaptation using asymmetric kernel transforms," in *CVPR 2011*. IEEE, 2011, pp. 1785–1792.
- [12] Y. Ganin, E. Ustinova, H. Ajakan, P. Germain, H. Larochelle, F. Laviolette, M. Marchand, and V. Lempitsky, "Domain-adversarial training of neural networks," *The Journal of Machine Learning Research*, vol. 17, no. 1, pp. 2096–2030, 2016.
- [13] E. Tzeng, J. Hoffman, K. Saenko, and T. Darrell, "Adversarial discriminative domain adaptation," in *Proceedings of the IEEE conference on computer vision and pattern recognition*, 2017, pp. 7167–7176.
- [14] M. Long, H. Zhu, J. Wang, and M. I. Jordan, "Unsupervised domain adaptation with residual transfer networks," in *Advances in neural information processing systems*, 2016, pp. 136–144.
- [15] Y. Ganin and V. Lempitsky, "Unsupervised domain adaptation by backpropagation," in *Proceedings of the 32nd International Conference on International Conference on Machine Learning-Volume 37*. JMLR.org, 2015, pp. 1180–1189.
- [16] Y. Chen, W. Li, C. Sakaridis, D. Dai, and L. Van Gool, "Domain adaptive faster r-cnn for object detection in the wild," in *Proceedings of the IEEE conference on computer vision and pattern recognition*, 2018, pp. 3339–3348.
- [17] X. Zhu, J. Pang, C. Yang, J. Shi, and D. Lin, "Adapting object detectors via selective cross-domain alignment," in *Proceedings of the IEEE Conference on Computer Vision and Pattern Recognition*, 2019, pp. 687–696.
- [18] T. Wang, X. Zhang, L. Yuan, and J. Feng, "Few-shot adaptive faster r-cnn," in *Proceedings of the IEEE Conference on Computer Vision and Pattern Recognition*, 2019, pp. 7173–7182.
- [19] K. Saito, Y. Ushiku, T. Harada, and K. Saenko, "Strong-weak distribution alignment for adaptive object detection," in *Proceedings of the IEEE Conference on Computer Vision and Pattern Recognition*, 2019, pp. 6956–6965.
- [20] Z. He and L. Zhang, "Multi-adversarial faster-rcnn for unrestricted object detection," in *Proceedings of the IEEE International Conference on Computer Vision*, 2019, pp. 6668–6677.
- [21] V. A. Sindagi, P. Oza, R. Yasarla, and V. M. Patel, "Prior-based domain adaptive object detection for hazy and rainy conditions," in *European Conference on Computer Vision*. Springer, 2020, pp. 763–780.
- [22] M. Hnewa and H. Radha, "Multiscale domain adaptive yolo for cross-domain object detection," in *IEEE International Conference on Image Processing (ICIP)*, 2021, pp. 3323–3327.
- [23] J. Redmon and A. Farhadi, "Yolo9000: better, faster, stronger," in *Proceedings of the IEEE conference on computer vision and pattern recognition*, 2017, pp. 7263–7271.
- [24] —, "Yolov3: An incremental improvement," *arXiv preprint arXiv:1804.02767*, 2018.
- [25] A. Bochkovskiy, C.-Y. Wang, and H.-Y. M. Liao, "Yolov4: Optimal speed and accuracy of object detection," *arXiv preprint arXiv:2004.10934*, 2020.
- [26] K. He, G. Gkioxari, P. Dollár, and R. Girshick, "Mask r-cnn," in *Proceedings of the IEEE international conference on computer vision*, 2017, pp. 2961–2969.
- [27] W. Li, F. Li, Y. Luo, P. Wang *et al.*, "Deep domain adaptive object detection: A survey," in *2020 IEEE Symposium Series on Computational Intelligence (SSCI)*. IEEE, 2020, pp. 1808–1813.
- [28] V. F. Arruda, T. M. Paixão, R. F. Berriel, A. F. De Souza, C. Badue, N. Sebe, and T. Oliveira-Santos, "Cross-domain car detection using unsupervised image-to-image translation: From day to night," in *2019 International Joint Conference on Neural Networks (IJCNN)*. IEEE, 2019, pp. 1–8.
- [29] C.-T. Lin, "Cross domain adaptation for on-road object detection using multimodal structure-consistent image-to-image translation," in *2019 IEEE International Conference on Image Processing (ICIP)*. IEEE, 2019, pp. 3029–3030.
- [30] T. Guo, C. P. Huynh, and M. Solh, "Domain-adaptive pedestrian detection in thermal images," in *2019 IEEE International Conference on Image Processing (ICIP)*. IEEE, 2019, pp. 1660–1664.
- [31] C. Devaguptapu, N. Akolekar, M. M Sharma, and V. N Balasubramanian, "Borrow from anywhere: Pseudo multi-modal object detection in thermal imagery," in *Proceedings of the IEEE/CVF Conference on Computer Vision and Pattern Recognition (CVPR) Workshops*, June 2019.
- [32] N. Inoue, R. Furuta, T. Yamasaki, and K. Aizawa, "Cross-domain weakly-supervised object detection through progressive domain adaptation," in *Proceedings of the IEEE conference on computer vision and pattern recognition*, 2018, pp. 5001–5009.
- [33] I. Goodfellow, J. Pouget-Abadie, M. Mirza, B. Xu, D. Warde-Farley, S. Ozair, A. Courville, and Y. Bengio, "Generative adversarial nets," in *Advances in neural information processing systems*, 2014, pp. 2672–2680.
- [34] C. Zhuang, X. Han, W. Huang, and M. Scott, "ifan: Image-instance full alignment networks for adaptive object detection," in *Proceedings of the AAAI Conference on Artificial Intelligence*, vol. 34, no. 07, 2020, pp. 13 122–13 129.
- [35] G. Zhao, G. Li, R. Xu, and L. Lin, "Collaborative training between region proposal localization and classification for domain adaptive object detection," in *European Conference on Computer Vision*. Springer, 2020, pp. 86–102.
- [36] H.-K. Hsu, C.-H. Yao, Y.-H. Tsai, W.-C. Hung, H.-Y. Tseng, M. Singh, and M.-H. Yang, "Progressive domain adaptation for object detection," in *The IEEE Winter Conference on Applications of Computer Vision*, 2020, pp. 749–757.
- [37] K. He, X. Zhang, S. Ren, and J. Sun, "Deep residual learning for image recognition," in *Proceedings of the IEEE conference on computer vision and pattern recognition*, 2016, pp. 770–778.
- [38] M. Everingham and J. Winn, "The pascal visual object classes challenge 2012 development kit," *Pattern Analysis, Statistical Modelling and Computational Learning, Tech. Rep*, 2011.
- [39] P. Sun, H. Kretzschmar, X. Dotiwalla, A. Chouard, V. Patnaik, P. Tsui, J. Guo, Y. Zhou, Y. Chai, B. Caine *et al.*, "Scalability in perception for autonomous driving: Waymo open dataset," in *Proceedings of the IEEE/CVF Conference on Computer Vision and Pattern Recognition*, 2020, pp. 2446–2454.
- [40] M. Khodabandeh, A. Vahdat, M. Ranjbar, and W. G. Macready, "A robust learning approach to domain adaptive object detection," in *Pro-*

- ceedings of the IEEE International Conference on Computer Vision*, 2019, pp. 480–490.
- [41] Q. Cai, Y. Pan, C.-W. Ngo, X. Tian, L. Duan, and T. Yao, “Exploring object relation in mean teacher for cross-domain detection,” in *Proceedings of the IEEE Conference on Computer Vision and Pattern Recognition*, 2019, pp. 11 457–11 466.
- [42] T. Kim, M. Jeong, S. Kim, S. Choi, and C. Kim, “Diversify and match: A domain adaptive representation learning paradigm for object detection,” in *Proceedings of the IEEE Conference on Computer Vision and Pattern Recognition*, 2019, pp. 12 456–12 465.
- [43] M. Xu, H. Wang, B. Ni, Q. Tian, and W. Zhang, “Cross-domain detection via graph-induced prototype alignment,” in *Proceedings of the IEEE/CVF Conference on Computer Vision and Pattern Recognition*, 2020, pp. 12 355–12 364.
- [44] A. Geiger, P. Lenz, and R. Urtasun, “Are we ready for autonomous driving? the kitti vision benchmark suite,” in *Conference on Computer Vision and Pattern Recognition (CVPR)*, 2012.